ISSN 0030-400X, Optics and Spectroscopy, 2019, Vol. 126, No. 3, pp. 290–293. © Pleiades Publishing, Ltd., 2019.
Russian Text © M.V. Tareeva, V.A. Dravin, R.A. Khmelnitskii, N.V. Chernega, A.D. Kudryavtseva, M.A. Shevchenko, A.O. Litvinova, 2019, published in Optika i Spektroskopiya, 2019, Vol. 126, No. 3, pp. 370–373.

BIOPHOTONICS

Stimulated Low-Frequency Raman Scattering in a Single-Crystal Diamond with a Buried Graphitized Layer

M. V. Tareeva[a, *], V. A. Dravin[a], R. A. Khmelnitskii[a], N. V. Chernega[a], A. D. Kudryavtseva[a], M. A. Shevchenko[a], and A. O. Litvinova[a, b]

[a] *Lebedev Physical Institute of the Russian Academy of Sciences, Moscow, 119991 Russia*

[b] *All-Russian Grabar' Art Research and Restoration Center, Moscow, 105005 Russia*

**e-mail: tareeva@sci.lebedev.ru*

Received October 10, 2018; revised October 10, 2018; accepted November 6, 2018

Abstract—The results of experimental observation of stimulated low-frequency Raman scattering (SLFRS) in a single-crystal diamond with a buried graphitized layer created as a result of nonlinear interaction of high-power nanosecond laser pulse with eigen oscillations of nanosized layers of diamond-graphite structures are presented. It is demonstrated that the frequency shift of the SLFRS is on the order of 10 GHz and is inversely proportional to geometrical dimensions of the nanolayers composing the structure.

DOI: 10.1134/S0030400X19030226

INTRODUCTION

Low-frequency Raman scattering experimentally observed for the first time in 1986 [1] represents one of the numerous optical effects observed in nanosized systems. An induced analog of this effect, namely, the stimulated low-frequency Raman scattering (SLFRS), has been observed for the first time by the authors of the present study [2].

The physical mechanism of the SLFRS is similar to that of the stimulated Raman scattering (SRS) by molecules where scattering takes place due to fluctuations of the dipole moment induced in the molecules (in nanoparticles, in the case of the SLFSR) by the fields of the pump and scattered radiation. Upon excitation of the medium by a high-power laser pulse, oscillations of nanoparticles are coherently driven by the pump and scattered fields. In so doing, the scattered wave has the form of a wave of spontaneous Raman scattering by thermal fluctuations of size and shape. The highest conversion efficiency of the pump radiation into an acoustic excitation of the medium is determined by the relation between the frequencies of the incident radiation and eigen oscillations and can be as high as 10^{-3}.

The SLFRS represents the so-called "q-independent type of scattering"; i.e., the SLFRS components can propagate forth forward or backward, i.e., copropagate or counterpropagate with the pump wave. This means that the frequency shift is independent of the angle between the wave vectors of the pump and scattered light waves, in contrast to light scattering from acoustic phonons in a homogeneous medium (e.g., Mandestam–Brillouin scattering). By changing the excitation conditions, it is thus possible to change the conversion efficiency of the SLFRS for forward and backward scattering.

When the driven mode is Raman active (e.g., in the case of inversion symmetry), it reveals itself in the SLFRS spectrum.

Theoretical estimates show that the frequency of the generated terahertz radiation under coherent excitation of an ensemble of nanoparticles at frequencies of eigen acoustic oscillations by a pulsed laser radiation must be inversely proportional to the size of the nanoparticles; i.e., the SLFRS frequency is determined by the morphology of the objects being excited and falls into the interval between several gigahertz to a terahertz, depending on the type of the studied system. Hence, variation of size of the nanoparticles can be instrumental in controlling the frequency of the generated radiation.

The conversion efficiency of the pump wave into the SLFRS wave in ensembles of certain types of nanoparticles, dielectric fluorides of rare-earth elements in particular, reaches 20% [3]. The threshold of the effect is estimated to be in the range between 0.01 and 0.05 GW/cm^2 [2, 4].

Obviously, in so doing, terahertz electromagnetic radiation itself must be generated as well. However, generation of coherent electromagnetic radiation of the terahertz range under excitation of nonlinearly active media has not been observed so far.

Here, we present the results of experimental investigation of the stimulated low-frequency Raman scat-

tering of light in a single-crystal diamond with a buried graphitized layer that has not been observed before in diamond structures of this kind, neither in stimulated nor in spontaneous regimes of scattering.

PREPARATION OF SAMPLES

Micron-scale single-crystal diamond films were chosen as an active medium for excitation of nonlinear acoustooptic interaction due to their outstanding physicochemical properties matching the experimental requirements, namely, high values of elastic moduli of diamond, large Raman shift of the one-photon mode (1332 cm^{-1}), relatively large value of the refractive index among optically transparent media, and large values of the thermal conductivity coefficients. Experimental samples representing plates of single-crystal diamond (nitrogen concentration of less than 5×10^{18} cm^{-3}) were cut parallel to the {111} crystallographic plane and subjected to ion implantation and annealing [5] (Fig. 1).

In the discussed experiment, polished plates of single-crystal diamond were bombarded by ions of carbon $^{12}C^+$, helium $^4He^+$, and deuterium D^+ with energies of 350, 50, and 350 keV, respectively, at room temperature. Since ion implantation leads to radiation damage, subsequent annealing resulted in creation of a graphitized layer in the region of maximum action of radiation in which carbon atoms form sp^2-type bonds [5, 6]. The samples were annealed in vacuum for an hour at a temperature of 1480°C (1600°C for sample implanted with D^+ at an energy of 350 keV) and pressure of 10^{-3} Pa. Surface graphitization was etched away in $H_2SO_4 + K_2Cr_2O_7$ solution at a temperature of about 180°C.

In the regions in which the level of radiation damage was below the graphitization threshold, defects were created as well, but the crystal structure above the buried graphitized layer corresponded to high-quality single-crystal diamond after annealing.

The depth at which the graphitized layer was created and the thickness of the reconstructed single-crystal diamond layer above it were determined by a number of parameters of the implantation regime (such as the type and energy of ions, the dose of implantation) and could be controlled in the course of ion implantation. This made possible obtaining samples with different size of nanolayers of the diamond–graphite structure. Position of the graphitized layer and its thickness were estimated by using the Monte Carlo modeling [5] of the distribution of defect concentration.

EXPERIMENTAL RESULTS

Stimulated scattering in the films was induced by pulsed radiation of a Q-switched ruby laser (wavelength $\lambda = 694.3$ nm, pulse width $\tau = 20$ ns, spectral width $\Delta\nu = 0.015$ cm^{-1}, beam divergence of 3.5×10^{-4} rad, and maximum pulse energy $E_{max} = 0.3$ J) (Fig. 2).

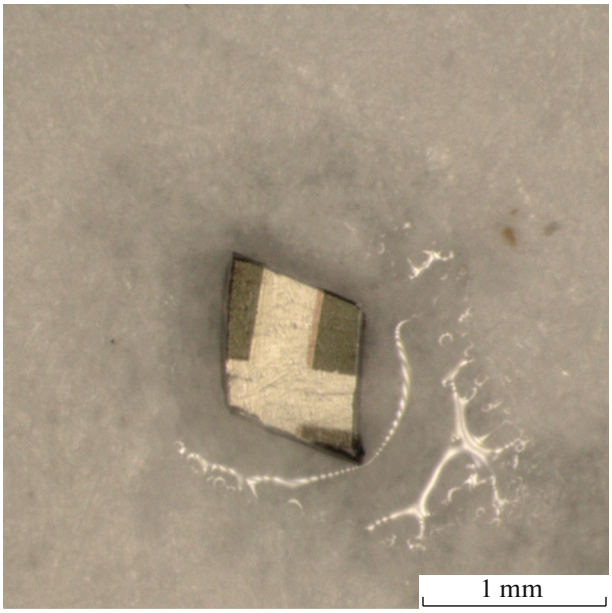

Fig. 1. An image of a single-crystal diamond film with graphitized layers obtained as a result of implantation of $^4He^+$ ions with an energy of 350 keV (annealing temperature of 1480°C) obtained by means of a digital Axiocam ICc 5 camera of an optical Carl Zeiss microscope. Dark areas on the sample (buried graphitized layers) correspond to different doses of ion implantation.

The laser radiation was focused on the sample surface at angles of 30°–60°. The power density in the sample was varied in the experiment by using lenses with differed focal lengths and by changing the pump-radiation energy.

A high-resolution Fabry–Perot interferometer with a cavity length variable in the 0.4–16.67 cm^{-1} range was used to measure fine structure of spectrum of the scattered radiation. The SLFRS revealed itself in the spectrum (in a Fabry–Perot interferogram) in the form of an intense additional (Raman) line in the Stokes region. The width and intensity of the SLFRS line were comparable with those of the anti-Stokes and Stokes lines of stimulated Raman scattering (SRS) observed earlier in a sample of single-crystal diamond with a buried graphitized layer obtained by means of implantation with helium ions with an energy of 180 keV.

The excitation threshold of the effect was 0.01 GW/cm^2. At this intensity, the peak conversion efficiency of the incident energy to SLFRS reached 40%.

The frequency shift of the SLFRS line from the laser line was 0.3 cm^{-1}, namely, 0.31 ± 0.01 cm^{-1} for the sample implanted with 50 keV $^4He^+$, 0.30 ± 0.01 cm^{-1} for the sample implanted with 0.30 ± 0.01 cm^{-1}, and 0.28 ± 0.01 cm^{-1} for the sample

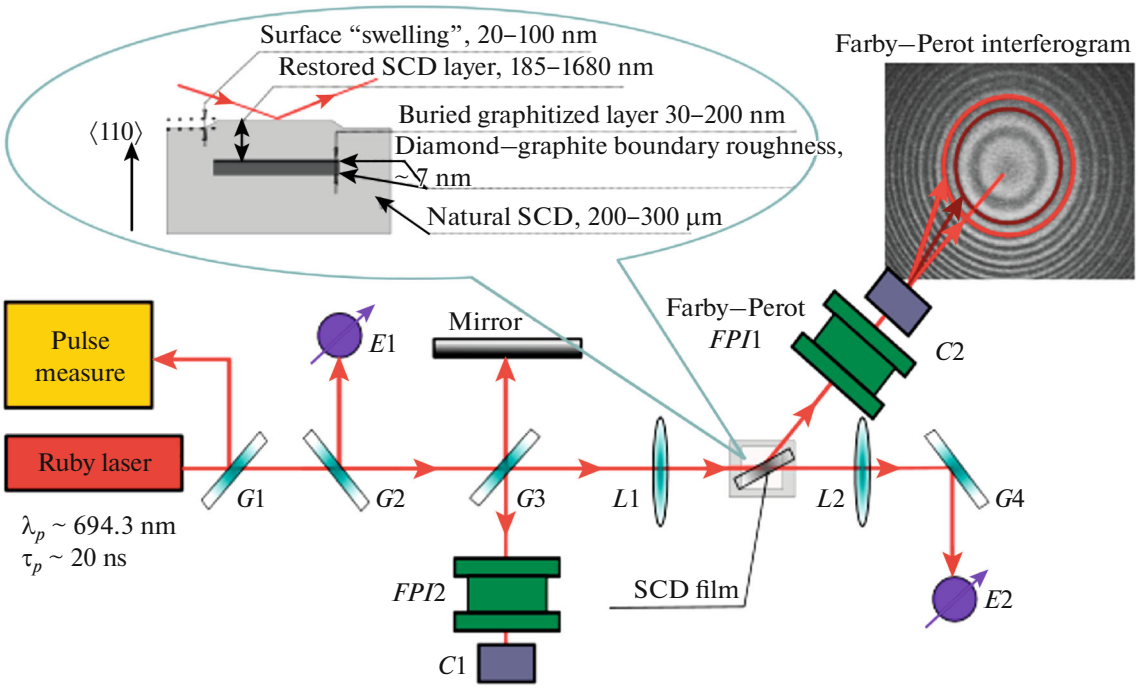

Fig. 2. Experimental layout. *G*1, *G*2, *G*3, and *G*4, glass plates; *E*1 and *E*, calibrated photodiodes for measuring scattered-light energy; Mirror, high reflector; *FPI*1 and *FPI*2, Fabry–Perot interferometers for analysis of the scattered light; *C*1 and *C*2, photodetectors; *L*1 and *L*2, lenses (focal distances of 3–10 cm), SCD film, a sample of a diamond film with a buried graphitized layer; Pulse measure, system of diagnostics of the pump-radiation parameters.

implanted with 350 keV D^+, or 9.3, 9, and 8.4 GHz, respectively (Table 1). For comparison, the values of the SLFRS frequencies observed in the bulk samples of synthetic opals made of silicon dioxide that represented three-dimensional structures consisting of densely packed SiO_2 globules with a diameter of several hundred nanometers are presented in Table 2. The SLFRS frequency shift was inversely proportional to the geometric parameters of the active scattering medium both for synthetic opals and single-crystal diamonds with a buried graphitized layer. This is because, in the classical approximation, the mode of eigen oscillations of the object is determined by its morphology (the shape and elastic properties) [7].

The low-frequency Raman shift of about 10 GHz is typical of nanostructures with the size of the scattering centers of several hundred nanometers [2, 3, 8–10], because the SLFRS frequency is inversely proportional to the diameter (size) of the nanoparticles exhibiting eigen oscillations in the direction along which the observed SLFRS mode propagates in the scattering object (a molecule, a virus, or a nanofilm).

In our experiments, such a dependence was observed as well: the SLFRS frequencies in a single-crystal diamond film were inversely proportional to the nanolayer dimensions (namely, the thickness of the graphitized later inside the diamond film and its depth, i.e., the thickness of the reconstructed single-crystal diamond film above it. We thus demonstrated for the first time that SLFRS can be observed not only in nanoparticles of different nature, including those forming a periodic solid-state nanostructure (e.g., in the case of synthetic opals), but also in nanostructured films in which an acoustic resonance involves eigen

Table 1. Comparison of characteristics of submicron single-crystal diamond films with a buried graphitized layer in which SLFRS was observed in the gigahertz frequency range

Energy and type of ions that bombarded diamond single crystal forming a graphitized layer	Dose of ion implantation, 10^{16} cm^{-2}	Depth of graphitized layer measured from the surface, nm	Graphitized layer thickness, nm	SLFRS frequency shift, GHz
50 keV $^4He^+$	2.5	185	84	9.3
350 keV $^{12}C^+$	0.4	365	100	9
350 keV D^+	12	1680	150	8.4

Table 2. Comparison of characteristics of bulk matrices of synthetic opals in which SLFRS was observed in the gigahertz frequency range

Spectral position of the peak in the spectrum of reflection, nm	Diameter of SiO_2 globules forming opal matrix, nm	SLFRS frequency shift, GHz
601.2	270	7.8
645.7	290	6.6
696.1	315	5.1

oscillations of the nanosystem consisting of a single-crystal diamond and a graphitized layer. A theory taking into account sound velocity in the graphitized layer and its elastic parameters, along with interaction of sound at an interface between the single-crystal diamond and the graphitized later, is needed for quantitative description of oscillations with frequencies on the order of 10 GHz.

CONCLUSIONS

A fundamental possibility of nonlinear excitation of a nanosized diamond structure leading to stimulated scattering in the gigahertz frequency range is demonstrated experimentally. It is shown that excitation of structures consisting of single-crystal diamond and graphite by pulsed laser radiation leads to generation of intense coherent radiation with a frequency shift on the order of 10 GHz that is typical for nanostructures with a size of several hundred nanometers. The value of the frequency shift of the stimulated low-frequency Raman scattering is determined by the morphology of the nanoparticles composing the nanosized system, namely, the frequencies of their eigen oscillations. Stimulated low-frequency Raman scattering of light thus represents a nonlinear-optical effect that enables obtaining not only high-intensity light scattering at the Stokes frequency, but also efficient coherent acoustic excitation of the gigahertz (possibly, also terahertz) frequency range directly by an optically active nanosized medium.

The results obtained in the present study can be used for creation of a source of coherent electromagnetic radiation of the terahertz range based on such diamond nanosystems.

For a number of complex molecules in which eigen frequencies of vibrational and rotational transitions lie in the terahertz frequency range, the SLFRS can be used for spectroscopic studies of materials containing such molecules.

High conversion efficiency of pump radiation to the Stokes wave can be used for obtaining a source of biharmonic pump for difference-frequency generation in the tera- and gigahertz frequency range.

ACKNOWLEDGMENTS

This research was supported by the Russian Foundation for Basic Research, project no. 16-32-60026 mol-a-dk.

REFERENCES

1. E. Duval, A. Boukenter, and B. Champagnon, Phys. Rev. Lett. **56**, 2052 (1986). doi 10.1103/PhysRevLett.56.2052
2. N. V. Tcherniega, M. I. Samoylovich, A. D. Kudryavtseva, A. F. Belyanin, P. V. Pashchenko, and N. N. Dzbanovski, Opt. Lett. **35**, 300 (2010). doi 10.1364/OL.35.000300
3. A. V. Safronikhin, H. V. Ehrlich, G. V. Lisichkin, A. D. Kudriavtseva, T. V. Mironova, M. A. Shevchenko, M. A. Strokov, N. V. Tcherniega, and K. I. Zemskov, J. Russ. Laser Res. **39**, 294 (2018). doi 10.1007/s10946-018-9721-5
4. M. V. Tareeva, V. A. Dravin, R. A. Khmelnitsky, A. D. Kudryavtseva, M. A. Strokov, M. A. Shevchenko, and K. A. Tsarik, J. Russ. Laser Res. **38**, 530 (2017). doi 10.1007/s10946-017-9676-y
5. A. V. Khomich, R. A. Khmelnitskiy, V. A. Dravin, A. A. Gippius, E. V. Zavedeev, and I. I. Vlasov, Phys. Solid State **49**, 1661 (2007). doi 10.1134/S1063783407090107
6. E. K. Nshingabigwi, T. E. Derry, S. R. Naidoo, J. H. Neethling, E. J. Olivier, J. H. O'Connell, and C. M. Levitt, Diamond Relat. Mater. **49**, 1 (2014). doi 10.1016/j.diamond.2014.07.010
7. M. Montagna, Phys. Rev. B **77**, 045418 (2008). doi 10.1103/PhysRevB.77.045418
8. N. V. Tcherniega, K. I. Zemskov, V. V. Savranskii, A. D. Kudryavtseva, A. Y. Olenin, and G. V. Lisichkin, Opt. Lett. **38**, 824 (2013). doi 10.1364/OL.38.000824
9. A. D. Kudryavtseva, N. V. Tcherniega, M. I. Samoylovich, and A. S. Shevchuk, Int. J. Thermophys. **33**, 2194 (2012). doi 10.1007/s10765-012-1259-0
10. O. V. Karpova, A. D. Kudryavtseva, V. N. Lednev, T. V. Mironova, V. B. Oshurko, S. M. Pershin, E. K. Petrova, N. V. Tcherniega, and K. I. Zemskov, Laser Phys. Lett. **13**, 085701 (2016). doi 10.1088/1612-2011/13/8/085701

Translated by I. Shumai